Available online at www.sciencedirect.com
ScienceDirect
Journal of the European Ceramic Society 30 (2010) 141–145
www.elsevier.com/locate/jeurceramsoc

Spontaneous fractal ordering of zirconium oxide nanoparticles during synthesis from solution

A.G. Belous [a], K.V. Kravchyk [a,*], O.V. Pashkova [a], Yu.P. Gomza [b], S.D. Nesin [b]

[a] *V. I. Vernadskii Institute of General and Inorganic Chemistry, Palladina Avenue 32/34, 03680, Kyiv – 142, Ukraine*
[b] *Institute of Chemistry of High-Molecular Compounds, UkraNational Academy of Sciences of Ukraine, Khar'kovskoe sh. 48, Kiev 02610, Ukraine*

Available online 18 July 2009

Abstract

The effect of synthesis conditions (pH of zirconium hydroxide precipitation) on the fractal structure of yttrium-stabilized zirconium oxide has been investigated. It has been found that the better pH of precipitation of zirconium hydroxide for obtaining soft-agglomerated nanoparticles ZrO_2 is ~4.5. It has been determined by small-angle X-ray scattering (SAXS) that the mass-fractal aggregation of precursors contributes to a good filtration of hydroxide precipitates and allows preparation of oxides with soft, readily destructible aggregates.

Keywords: Sol–gel processes; ZrO_2; Fractal structure

1. Introduction

Materials based on stabilized zirconium oxide are finding numerous applications in engineering as structural and functional materials.[1–4] An important problem is the degradation of powders and materials based on zirconium oxide.[5] The use of nanocrystalline powders for the production of bulk materials involves many specific problems deriving form the intense growth of particles with increasing temperature followed by the formation of strong internal deformations in the ceramics.

The interest is focused on the synthesis of nanoparticles of precursors in obtaining of nanocrystalline ceramics. However, nanoparticles not always guarantee the obtaining of nanocrystalline materials; this is connected with different degree of their self-organization. It is already known that nanoscale dispersions are inclined to the self-assembly of particles into ordered structures.[6,7] At the same time, the hierarchy of structure from primary clusters to conglomerate is formed.[8] In other words the processes of nanoparticles synthesis particularly of complex oxide systems (synthesis from solution, from gas medium, etc.) are realized under the conditions of open thermodynamic systems, which are characterized by spontaneous formation and evolution of complicated ordering of structures. Investigation of self-organization processes is important, which are playing the main role in obtaining of small crystalline ceramics and, thus, affect their properties appropriately. Current article is the sequel to our previous investigations[9] regarding the effect of conditions of obtaining of stabilized zirconium oxide on the processes of fractal self-organization, where it has been shown that using of different methods of obtaining of stabilized zirconium oxide (SPH and CPH) can affect appreciably not only the size but also the properties of the particles (their self-organization). In the current paper we have studied the pH influence of precipitation of zirconium hydroxide obtained by SPH on the fractal self-organization processes in order to determine the most appropriate pH for obtaining of weakly agglomerated nanoparticles of stabilized zirconium oxide.

2. Experimental procedure

We have chosen system $0.97ZrO_2 \cdot 0.03Y_2O_3$ as model object for studying of self-organization of stabilized zirconium oxide during the synthesis from solutions. The precursors were synthesized by the method of sequential precipitation of hydroxides (SPH). As initial salts 2 M aqueous solutions of $ZrOCl_2$ and $Y(NO_3)_3$ were used. $ZrO(OH)_2$ was precipitated at different magnitudes of pH (4; 4.5; 5; 6; 6.5). $Y(OH)_3$ was precipitated on preliminary precipitated $ZrO(OH)_2$. The precipitates were washed off from the mother solution with distilled water until there were no Cl^- and NO_3^- ions in the scourages. Air-dry xerogels and xerogels calcined at $T = 870$ K/1 h were investigated.

* Corresponding author. Tel.: +380 44 4242211; fax: +380 44 4242211.
E-mail address: krawtschyk@yahoo.com (K.V. Kravchyk).

0955-2219/$ – see front matter.
doi:10.1016/j.jeurceramsoc.2009.06.028

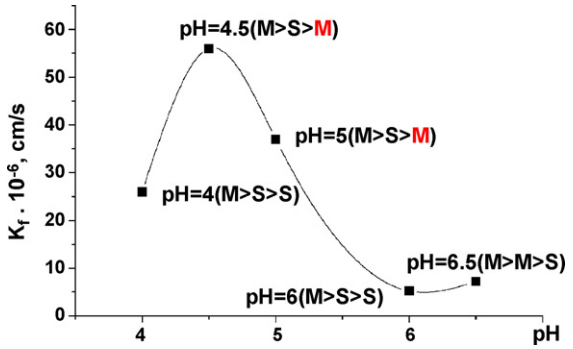

Fig. 1. pH of $ZrO(OH)_2$ precipitation dependence of the filtration coefficient (K_f) of precipitates.

X-ray powder diffraction experiments were carried out on a DRON-4-07 diffractometer at the room temperature using Cu Kα radiation and a step-scanning mode in the 2θ range from 10° to 150°, with a step size of 0.02°. The average crystallite size of the samples was estimated by Scherrer equation using the diffraction intensity of all prominent lines.[10] The particle size and morphology of annealed at $T = 600$ °C powders of stabilized zirconium oxide were determined using a scanning electron microscope JEM 10CXII (JEOL).

Small-angle X-ray scattering (SAXS) curves were obtained in a vacuum Kratky camera using a Cu-anode tube as the X-ray source. Recording of SAXS data has been performed in conditions of multiple scanning of scintillation detector in the region of scattering angles from 0.03° to 4.0° ($q = 4\pi \sin\theta/\lambda = 0.022$–$2.86\ \mathrm{nm}^{-1}$). Preliminary processing of SAXS curves was performed using FFSAXS[11] program. Also, procedures of deletion of parasitic scattering by the camera and cuvette windows, normalization of the scattered intensity to absolute units, and the introduction of the collimation correction have been used. For performing of SAXS experiments, studied materials in view of fine-dispersed powders were inserted in cuvettes 0.1–0.2 mm in thickness, with 17-μm-thick Mylar windows.

For modeling of profiles of SAXS curves, Beaucage's method of unified exponential functions was used.[12,13] The equation describing an arbitrary number of interrelated structural levels has the following view:

$$I(q) = \sum_{i=1}^{n} \left(G_i \exp\left(\frac{-q^2 R_{g_i}^2}{3}\right) + B_i \exp\left(\frac{-q^2 R_{g_{(i+1)}}^2}{3}\right) \times \left\{ \frac{[erf(qR_{g_i}/6^{1/2})]^3}{q} \right\}^{-P_i} \right) \quad (1)$$

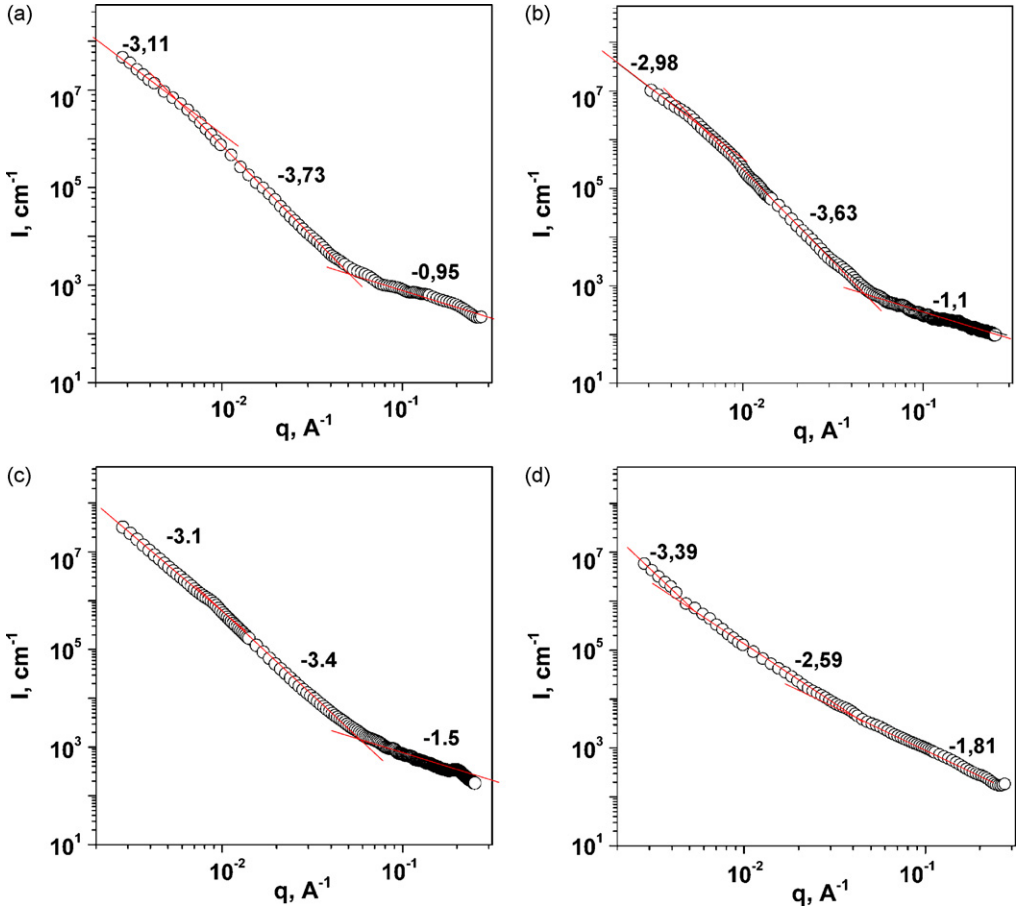

Fig. 2. Small-angle X-ray scattering curves of air-dry samples obtained at different pH of zirconium hydroxide precipitation: (a) 4; (b) 4.5; (c) 5; (d) 5.5; I is intensity; q is wave vector.

where G_i is the coefficient at Guinier ratio for level i, R_{g_i} is the radius of gyration of fractal aggregates at level i, B_i is coefficient at the Porod factor for power dependence of the logarithm of the scattered intensity on the logarithm of the scattering vector, and P_i is the exponent defining the fractal dimension of aggregates at level i ($1 < P < 3$ for mass and $3 > P > 4$ for surface fractals). The mass-fractal dimension is $D_s = P$, and the surface-fractal dimension is $D_s = 6 - P$.

3. Results and discussion

Fig. 1 shows pH of $ZrO(OH)_2$ precipitation dependence of the filtration coefficients (K_f) of precipitates. As it is obvious from Fig. 1, the filtration coefficients of precipitates differ essentially depending on the pH of precipitations of $ZrO(OH)_2$. The precipitations, which had high filtration coefficients, were characterized by weak bonds between particles. It has showed itself in friability of air-dry and calcined powders.

Fig. 2(a)–(c) shows SAXS curves of air-dry samples at different pH of zirconium hydroxide precipitation. The results of modeling of experimental data are listed in Table 1. It can be seen from Fig. 2 that the curves are characterized by three linear regions (straight-line segments), over which the corresponding slope angle values are given. The type of fractal aggregation for each region and fractal dimension was determined from the slope angle of such regions.

As it can be seen from the result presented (Fig. 2 and Table 1), the xerogels of all samples are characterized at the first lowest aggregation level (the range of maximum q values and hence minimum values of dimensions) by the presence of mass fractals (primary particles of fractal object) with the radii of rotation $R_g = 2.5$–4.34 nm and fractal dimension $D = 0.62$–1.81. This corresponds to the formation, at the first dimensional level, of oblong particles with a mean diameter of $d = 6.5$–11.2. The change of the slope of SAXS curves (Fig. 2) and the increase of fractal dimension are associated with the aggregatability of primary particles into surface fractals of larger size (see Table 1).

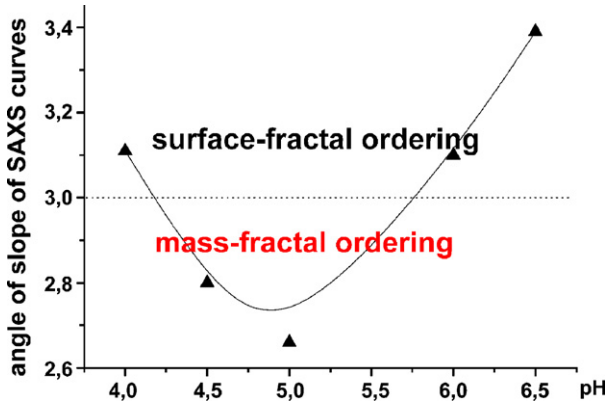

Fig. 3. pH of $ZrO(OH)_2$ precipitation dependence of angle of slope of SAXS curves on third agglomeration level.

Surface fractals form at a higher (third) structure level mass or surface fractals with the different magnitudes of diameters depend on pH of $ZrO(OH)_2$ precipitation.

The sequence of the fractal aggregation types of xerogels (starting from the lowest level) is as follows: M → S → M(S) for all samples. Depending on the pH of zirconium hydroxide precipitation, mass and surface fractals can be formed on the third aggregation level. As it can be seen from Fig. 3, changing of the pH of zirconium hydroxide precipitation leads to the changing of the fractal aggregation type on the third structure level. Mass-fractal and surface-fractal agglomerates are formed in regions pH ≈ 4.25–5.75 and pH ≤ 4, pH ≥ 6.

Thereby, the influence of pH of precipitation of hydroxides on the type of fractal aggregation affects the third structure level. Taking into account the difference in the structure of mass and surface fractals (Fig. 4) and pH of $ZrO(OH)_2$ precipitation dependence of the filtration coefficient (K_f), one can understand why the filtration coefficient of samples obtained at pH = 4.5, 5 is higher K_f of samples obtained at pH = 4, 5.5, 6. During the filtration of hydroxide precipitates with surface-fractal aggregation, the water will easily pass through the surface layer and will

Table 1
Structural parameters determined by fitting the SAXS curves of xerogels.

Sample	Structural level	Fractal type	s	D	R_g (nm)	D_s (nm)
pH = 4	1	M	−0.95	0.95	3.65	9.4
	2	S	−3.73	2.27	20	51.6
	3	S	−3.11	2.89	175	451.5
pH = 4.5	1	M	−1.1	1.1	3.0	7.74
	2	S	−3.63	2.37	30	77.4
	3	M	−2.8	2.8	130	335.4
pH = 5.0	1	M	−0.62	0.62	4.34	11.2
	2	S	−3.86	2.14	15.38	39.7
	3	M	−2.66	3.34	227	585.7
pH = 6.0	1	M	−1.5	1.5	2.5	6.5
	2	S	−3.4	2.6	22	56.8
	3	S	−3.1	2.9	150	387
pH = 6.5	1	M	−1.81	1.81	4	10.3
	2	M	−2.59	2.59	44	113.5
	3	S	−3.39	2.61	263	678.5

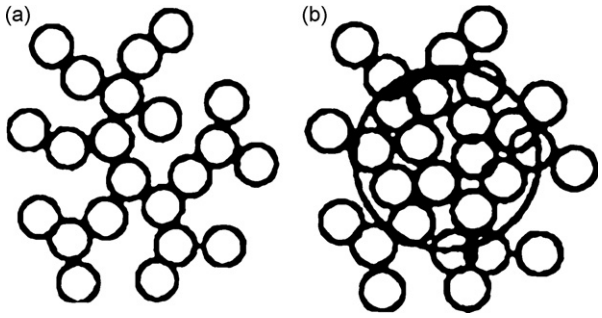

Fig. 4. Schematic drawing of mass-fractal (a) and surface fractal (b) aggregates.[14]

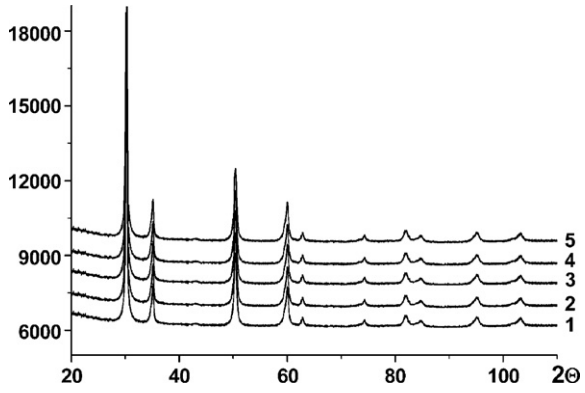

Fig. 5. Diffractograms of calcined samples at $T = 600\,^{\circ}C/1$ h: (1) 4; (2) 4.5; (3) 5; (4) 5.5; (5) 6.

linger in the bulk. The precipitates with mass-fractal aggregation have a loose structure in the whole volume and, therefore, water passes easily through the precipitate layer at a high rate. It should be noted that xerogels obtained at pH = 4.5, 5 are characterized by weak bonds between particles in comparison with xerogels obtained at pH = 4, 5.5, 6, 6.5. This manifest itself by the friability of the former (aggregates of particles where mass fractals are formed on third agglomeration level, are easy to break up through the light pressure on them, whereas a certain force is required to crush surface-fractal agglomerates). It is important

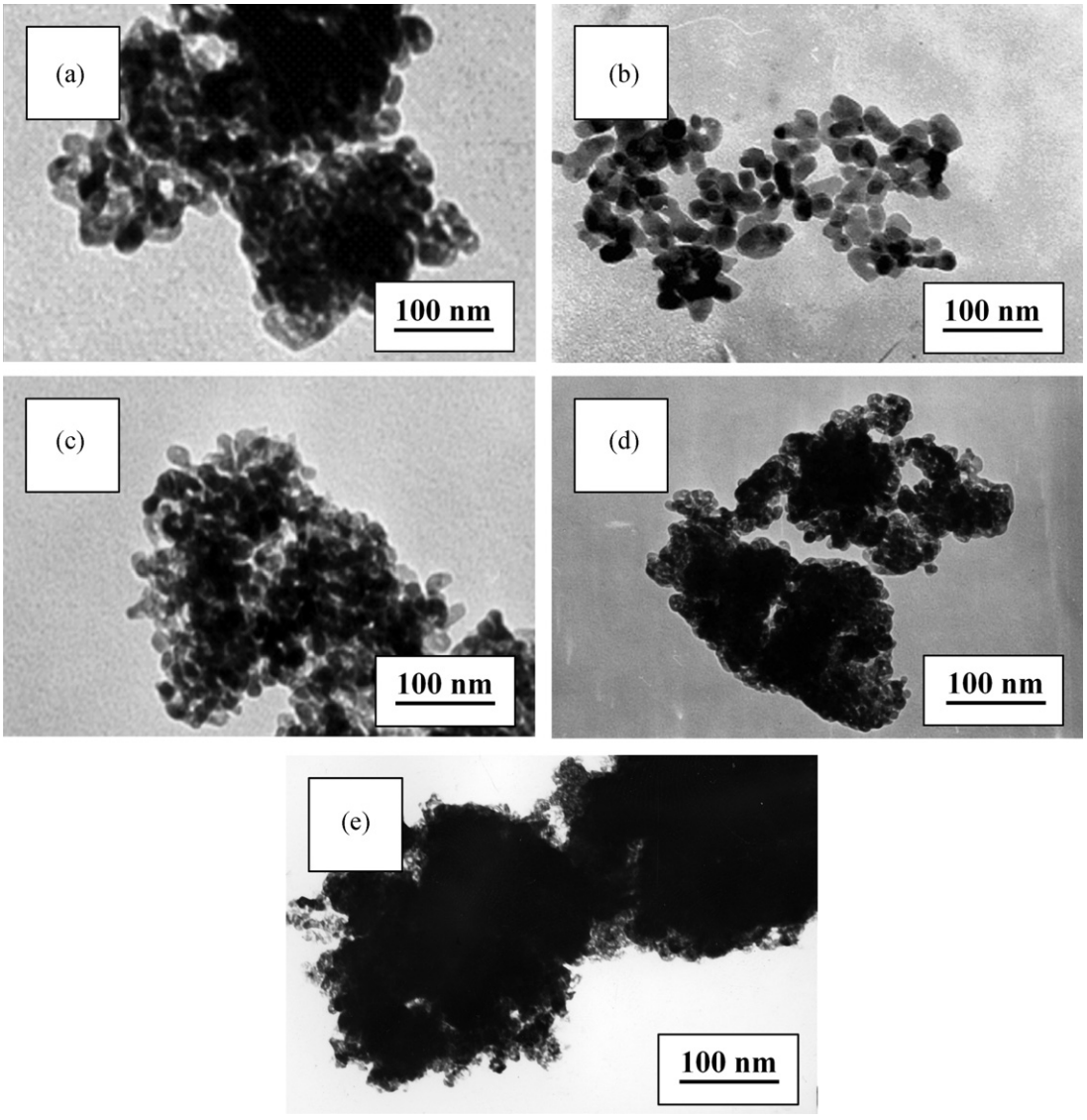

Fig. 6. Microphotographs of calcined samples at $T = 600\,^{\circ}C/1$ h obtained at different pH of zirconium hydroxide precipitation: (a) 4; (b) 4.5; (c) 5; (d) 5.5; (e) 6.

to note that similar results were obtained during the investigation of precipitates of stabilized zirconium oxide obtained by the methods of sequential precipitation and co-precipitation of the hydroxides.[9]

Calcined xerogels (600 °C/1 h) of all samples are characterized by single-phase fluorite-type cubic crystal structure (Fig. 5) with the same lattice parameters. However, ZrO_2 samples (as well as corresponding xerogels) differ sharply in the strength of aggregates (agglomerates). This is confirmed by electron microscopy data (Fig. 6). As it can be seen from Fig. 3, samples with mass-fractal agglomeration ($pH_{ZrO(OH)_2} = 4.5$; 5) are characterized by the lowest agglomerability in contrast to samples with surface-fractal agglomeration ($pH_{ZrO(OH)_2} = 4$; 5.5; 6; 6.5). Thus, in case of forming of mass fractals in xerogels on the third agglomeration level, calcined precipitates have low agglomeration. Thus, the self-assembly of particles in precursors determines the technological properties of ZrO_2-based oxides. There results demonstrate clearly the manifestation of the effect of topochemical memory.[6]

As results of investigations have shown, nanoparticles have similar sizes, but they are characterized at the same time by different properties. Undoubtedly, the size of particles is an important feature, but this factor alone is not enough, because there are a lot of various reasons that affect properties of materials. Particularly, one of such reasons is fractal structure formed during the synthesis of nanoparticles.

4. Conclusions

At the synthesis from solutions of materials of ZrO_2–Y_2O_3 system, the correlation nature of precursor-type of fractal aggregation-technological properties of ZrO_2 powders has been established. It has been shown that the mass-fractal aggregation of precursors contributes to a good filtration of hydroxide precipitates and allows preparation of oxides precursor with soft, readily destructible aggregates. It has been found that the better pH of precipitation of zirconium hydroxide for obtaining soft-agglomerated nanoparticles ZrO_2 is ∼4.5.

References

1. Okada, A., Automotive and industrial applications of structural ceramics in Japan. *J. Eur. Ceram. Soc.*, 2008, **28**, 1097–1104.
2. Kelly, J. R. and Denry, I., Stabilized zirconia as a structural ceramic: an overview. *Dent. Mater.*, 2008, **24**, 289–298.
3. Lee, J. H., Kim, J., Kim, S. W., Lee, H. W. and Song, H. S., Characterization of the electrical properties of Y_2O_3-doped CeO_2-rich CeO_2–ZrO_2 solid solutions. *Solid State Ionics*, 2004, **166**, 45.
4. Kawamura, K., Watanabe, K., Hiramatsu, T., Kaimai, A., Nigara, Y., Kawada, T. and Mizusaki, J., Electrical conductivities of CaO doped ZrO_2–CeO_2 solid solution system. *Solid State Ionics*, 2001, **144**, 11.
5. Butz, B., Kruse, P., Störmer, H., Gerthsen, D., Müller, A., Weber, A. and Ivers-Tiffée, E., Correlation between microstructure and degradation in conductivity for cubic Y_2O_3-doped ZrO_2. *Solid State Ionics*, 2006, **177**, 3275–3284.
6. Tretyakov, Yu. D., Self-organisation processes in the chemistry of materials. *Russ. Chem. Rev.*, 2003, **72**, 651.
7. Roldughin, V. I., Self-assembly of nanoparticles at interfaces. *Russ. Chem. Rev.*, 2004, **73**, 115.
8. Shpak, A. P., Cheremskoi, P. G., Kunitskii, Yu. A. and Sobol, O. V., Klasternye i nanostructurnye materially. *Kiev, Part 3*, 2005, 142.
9. Kravchik, K. V., Gomza, Yu. P., Pashkova, O. V., Belous, A. G. and Nesin, S. D., Effect of zirconium and yttrium hydroxide precipitation conditions on the fractal structure of the resulting xerogels and $0.97ZrO_2{\cdot}0.03Y_2O_3$ powders. *Inorg. Mater.*, 2007, **43**, 258–263.
10. Klug, H. P. and Alexander, L. E., *X-ray Diffraction Procedures*. Wiley-Interscience, New York, 1974, p.125.
11. Vonk, C. G., *FFSAXS's Program for the Processing of Small-angle X-ray Scattering Data*. DSM, Geleen, 1974, p. 83.
12. Beaucage, G., Small-angle scattering from polymeric mass fractals of arbitrary mass-fractal dimension. *J. Appl. Crystallogr.*, 1996, **29**, 134–146.
13. Hyeon-Lee, J., Beaucage, G., Prausnits, S. E. and Vemury, S., Fractal analysis of flame-synthesized nanostructured silica and titania powders using small-angle X-ray scattering. *Langmuir*, 1998, **14**, 5751–5756.
14. Shpak, A. P., Shilov, V. V., Shilova, O. A. and Kunitskii, Yu. A., Diagnostika nanosistem. Mnogourovnevye fraktal'nye nanostruktury. *Kiev, Part 2*, 2004, 111.